

Electronic Correlations and Multiorbital Effects in Iron Pnictides and Chalcogenides

Rong Yu

Renmin University of China

Sep. 24 , 2014



Collaborators

Theory

Emilian Nica (Rice)

Wenxin Ding (Rice)

Qimiao Si (Rice)

Jian-Xin Zhu (LANL)

ARPES

Ming Yi (Berkeley)

Donghui Lu (SLAC)

Zhi-Xun Shen (Stanford)

Neutron Scattering

Chenglin Zhang (Rice)

Pengcheng Dai (Rice)

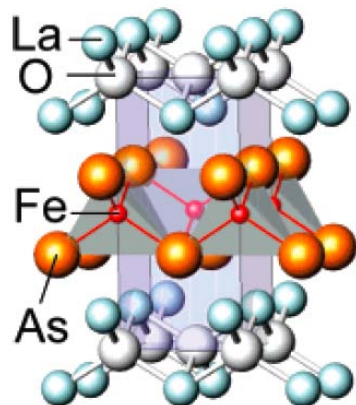
Outline

- Introduction--electron correlations in iron-based superconductors
- Metal-insulator transition in multiorbital models for iron-based superconductors
 - Slave-spin formulation for multi-orbital models
 - Mott transitions in iron pnictides: phase diagram
 - Alkaline iron selenides: Mott localization and orbital-selective Mott phase
- Pairing amplitudes: orbital selective pairing
- Summary

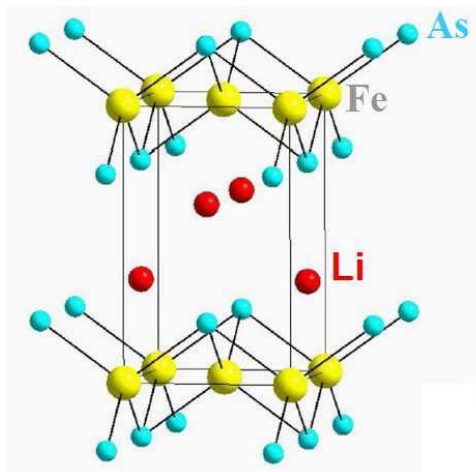
Family of Iron Based Superconductors

pnicides:

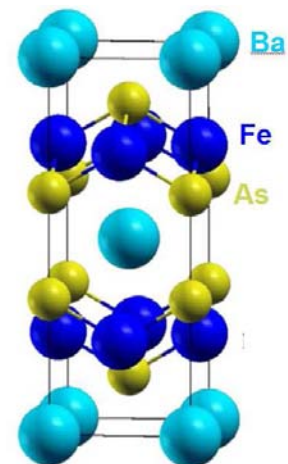
1111: LaOFeAs



111: LiFeAs

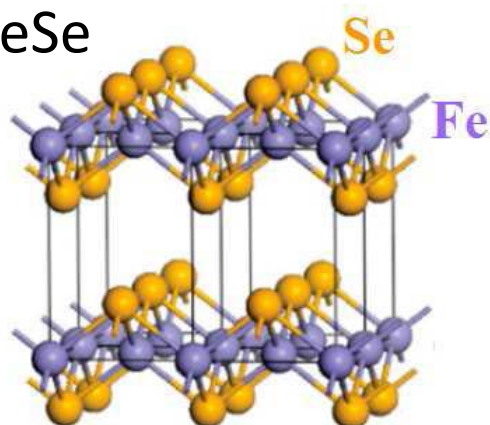


122: BaFe₂As₂

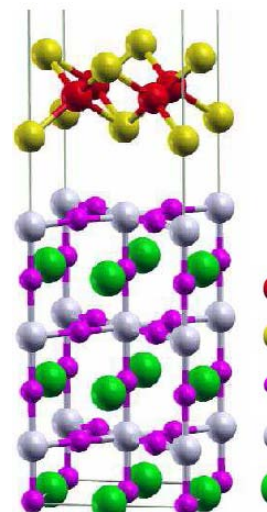


chalcogenides:

11: FeSe

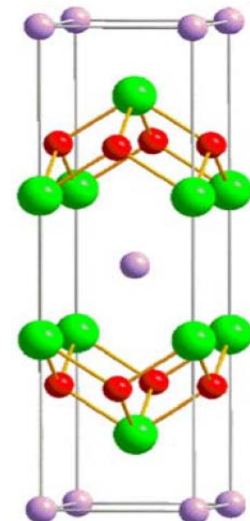


1-layer
FeSe



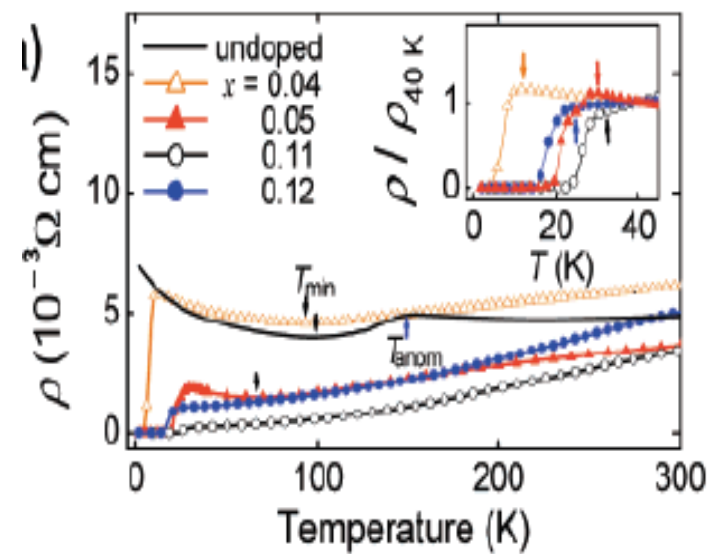
$A_xFe_{2-y}Se_2$

■ Fe
■ Se
● O
● Ti
● Sr

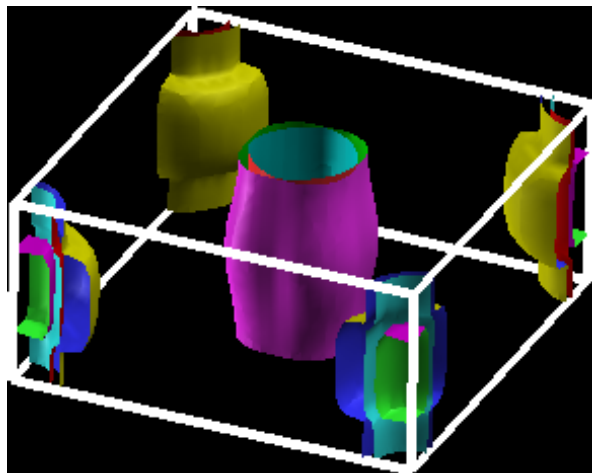


● K
● Fe
● Se

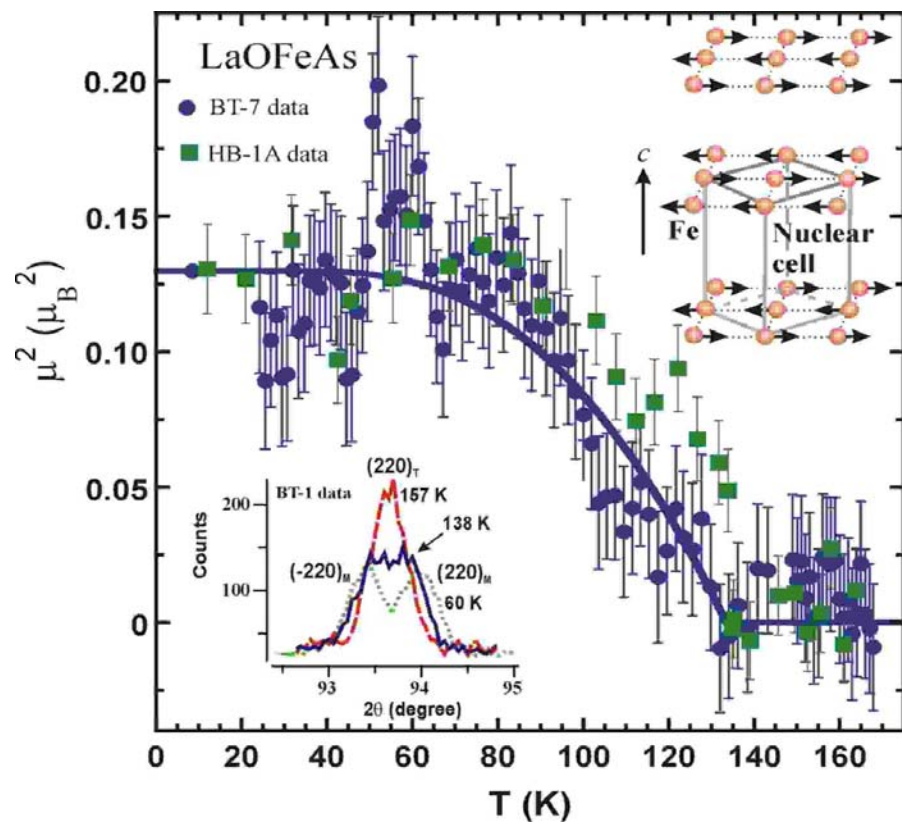
Parent Pnictides: Electronic Properties



Kamihara et al, JACS **130**, 3296 (2008)



Singh & Du, PRL **100**, 237003 (2008)



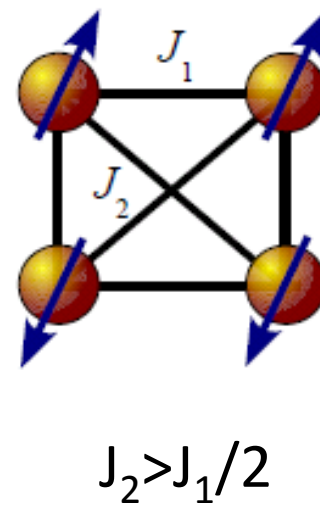
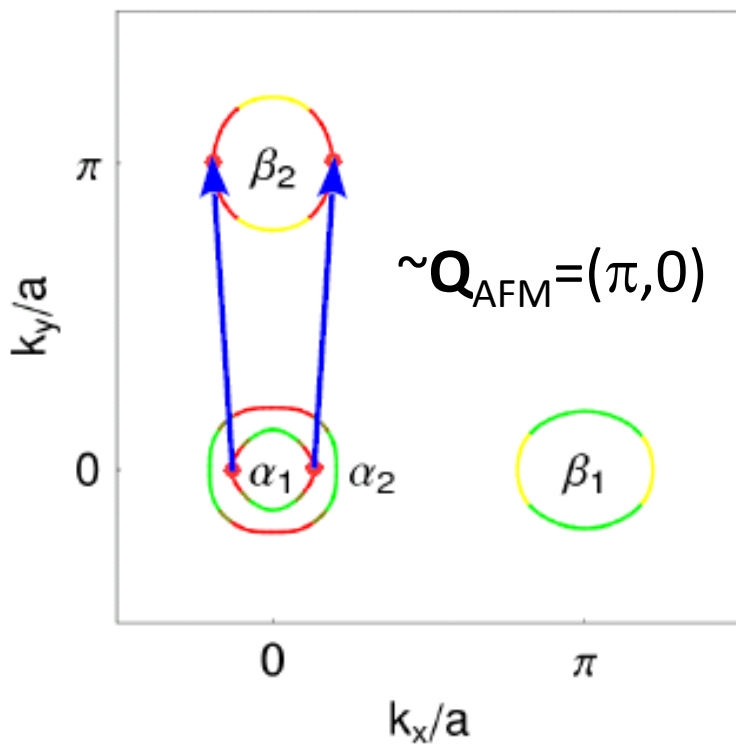
de la Cruz et al., Nature **453**, 899 (2008)

columinar $(\pi, 0)$ antiferromagnetic metal with small electron & hole pockets

Understanding the Magnetic Order in Iron Pnictides

weak coupling:
Fermi surface nesting

strong coupling:
Interacting local moments

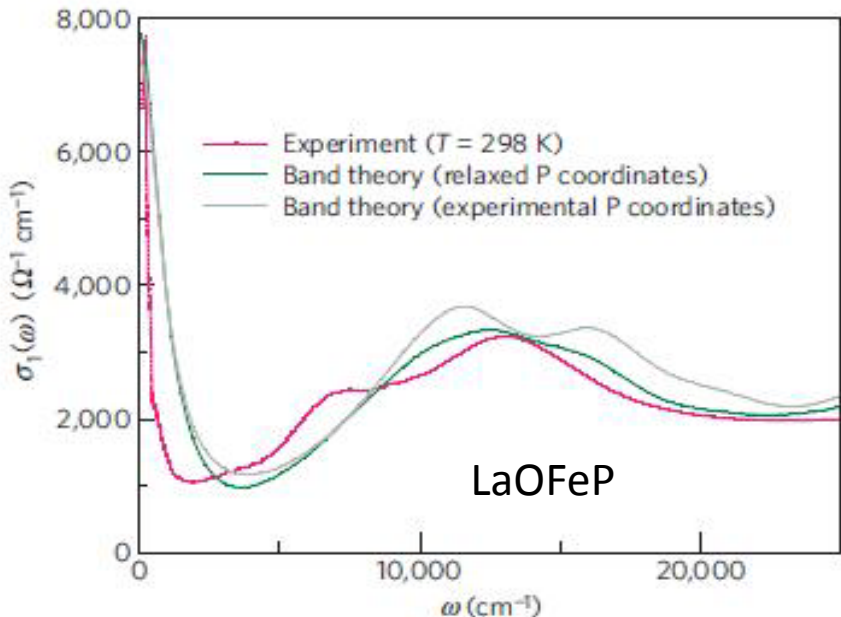


Evidence for Electron Correlations

Bad metal behavior of the parent compound

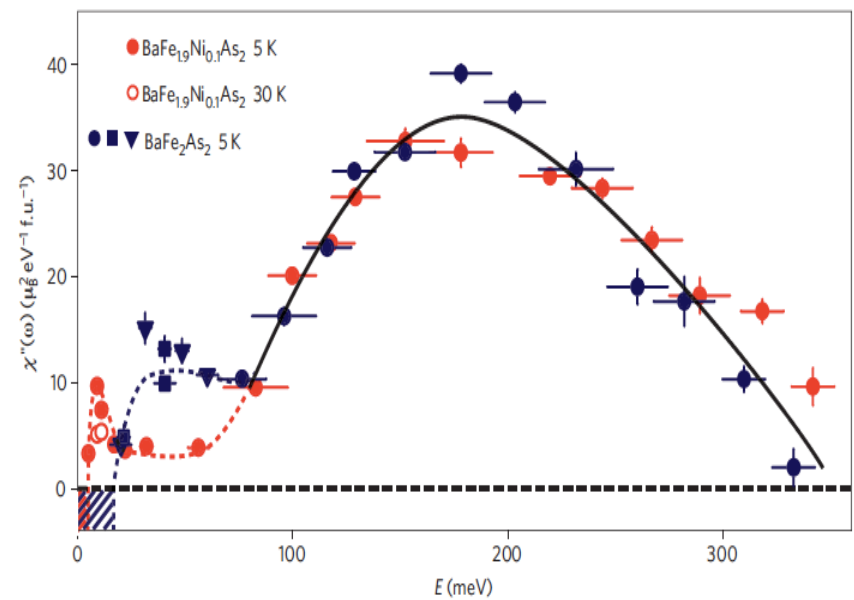
- ✓ Transport: large room-T resistivity, reaches the Ioffe-Regel limit
- ✓ Spectroscopy:

reduction of Drude weight



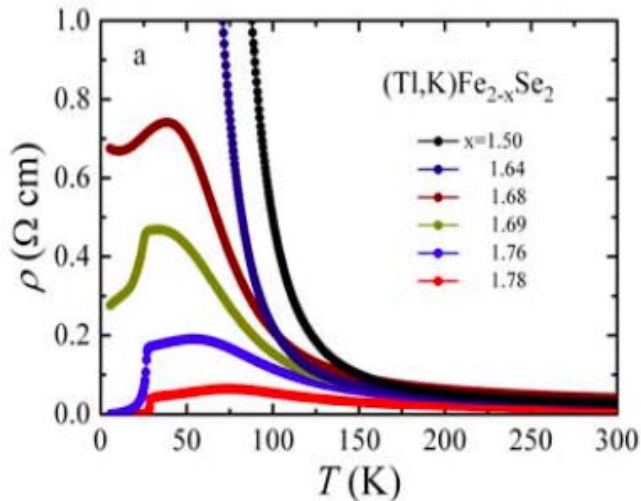
Qazilbash et al, Nat. Phys. 5, 647 (2009)

large overall spin spectral weight

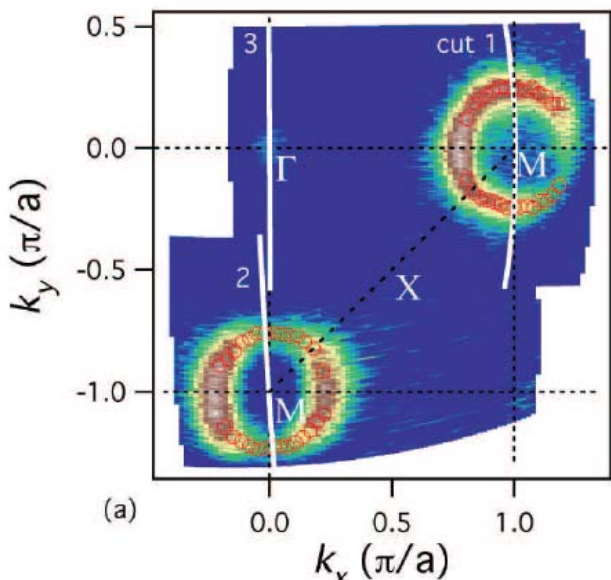


Liu et al, Nat. Phys. 8, 376 (2012)

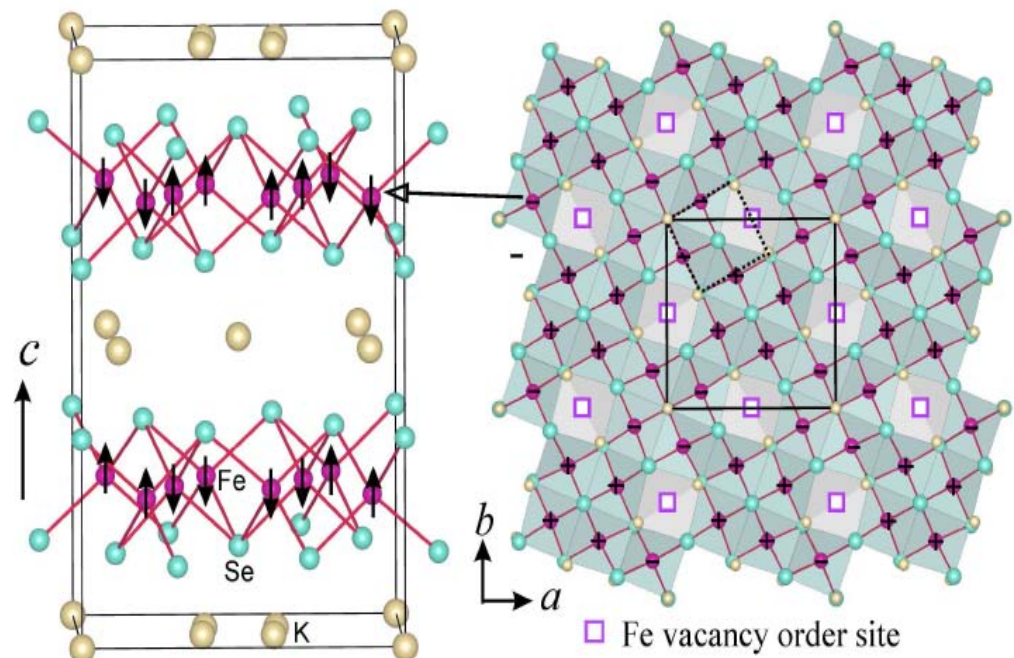
Properties of Alkaline Iron Selenides



Fang et al, EPL **94**, 27009 (2011)



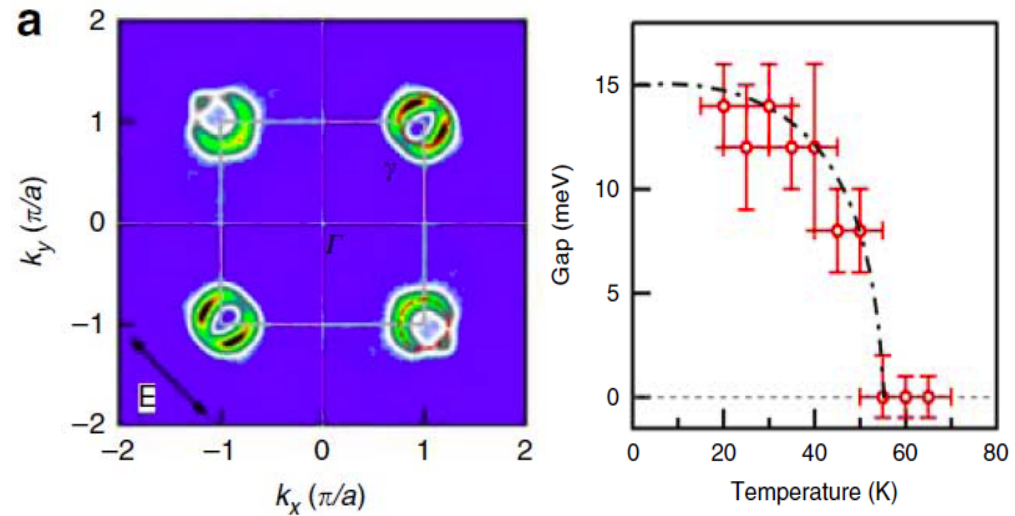
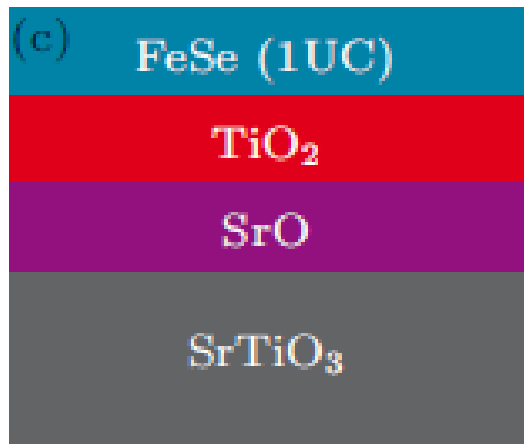
Qian et al., PRL **106**, 187001 (2011)



Bao et al., CPL **28**, 086104 (2011)

- Metallic/Insulating, depending on Fe content
- Fermi surface: electron pockets only
- Magnetic order influenced by ordered Fe vacancies

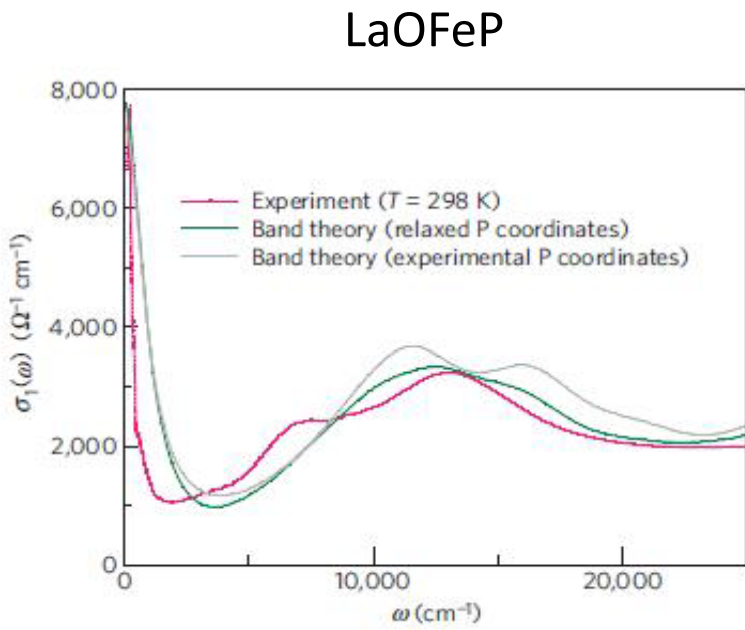
Properties of Single-Layer FeSe/SrTiO₃



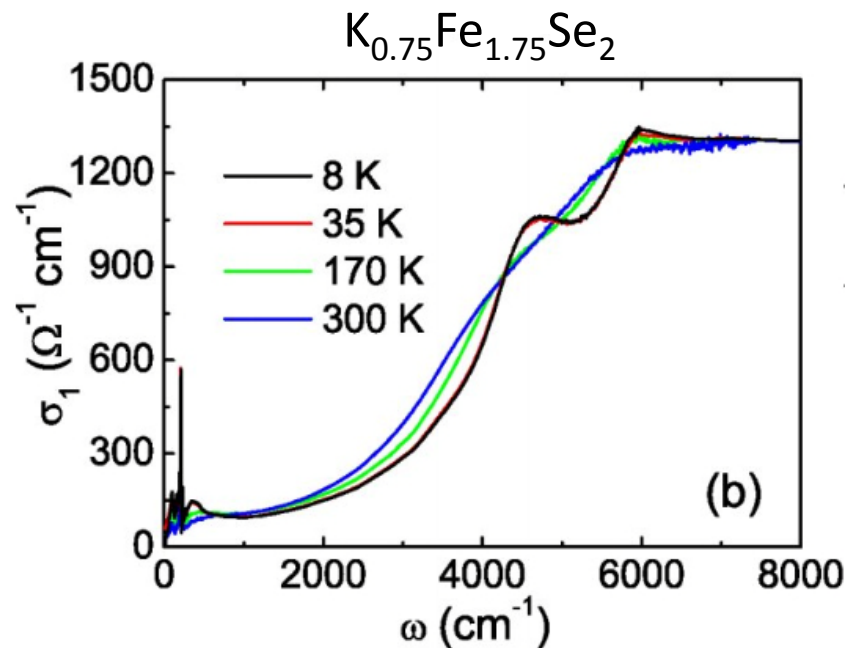
Liu et al., Nat. Comm. **3**, 931 (2012).

- ✓ Electron pockets only
- ✓ $T_c >= 60$ K from ARPES, STM and transport measurements

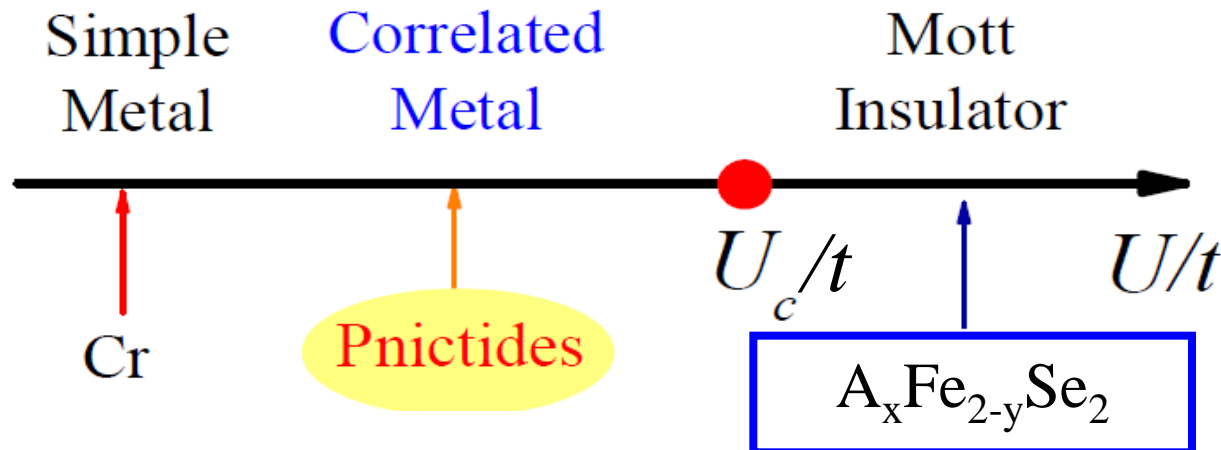
Electron Correlations and Mott Localization



Qazilbash et al, Nat. Phys. **5**, 647 (2009)



Yuan et al., Sci. Rep. **2**, 221 (2012).



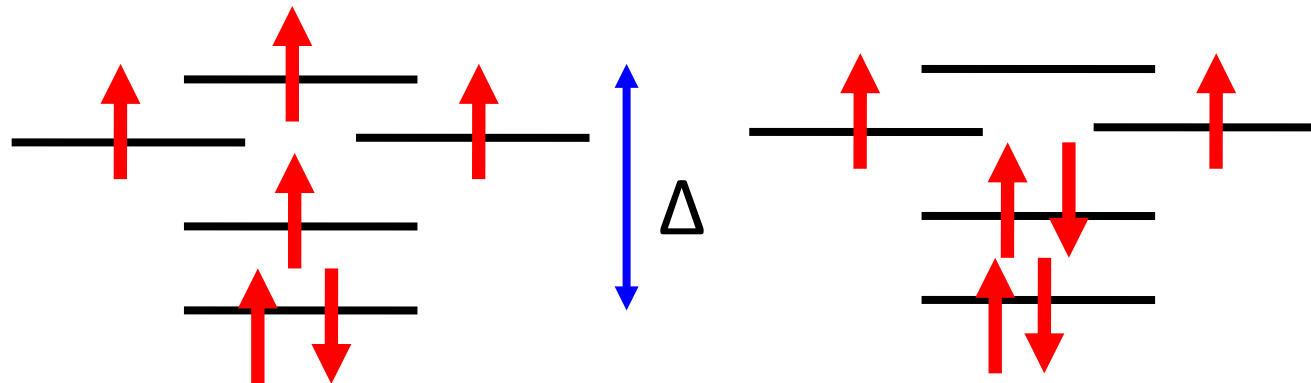
How will the Mott transition take place in the multi-orbital iron-based systems with even number of electrons per unit cell?

Multi-Orbital Hubbard Model

$$H = H_{\text{TB}} + H_{\text{int}}$$

$$\begin{aligned} H_{\text{int}} = & U \sum_{\mathbf{i}, \alpha} n_{\mathbf{i}, \alpha, \uparrow} n_{\mathbf{i}, \alpha, \downarrow} + \left(U' - \frac{J}{2} \right) \sum_{\mathbf{i}, \alpha < \beta} n_{\mathbf{i}, \alpha} n_{\mathbf{i}, \beta} \\ & - 2J \sum_{\mathbf{i}, \alpha < \beta} \mathbf{S}_{\mathbf{i}, \alpha} \cdot \mathbf{S}_{\mathbf{i}, \beta} - J \sum_{\mathbf{i}, \alpha < \beta} (d_{\mathbf{i}, \alpha, \uparrow}^\dagger d_{\mathbf{i}, \alpha, \downarrow}^\dagger d_{\mathbf{i}, \beta, \uparrow} d_{\mathbf{i}, \beta, \downarrow} + \text{H.c.}) \end{aligned}$$

Systems filled with even electrons



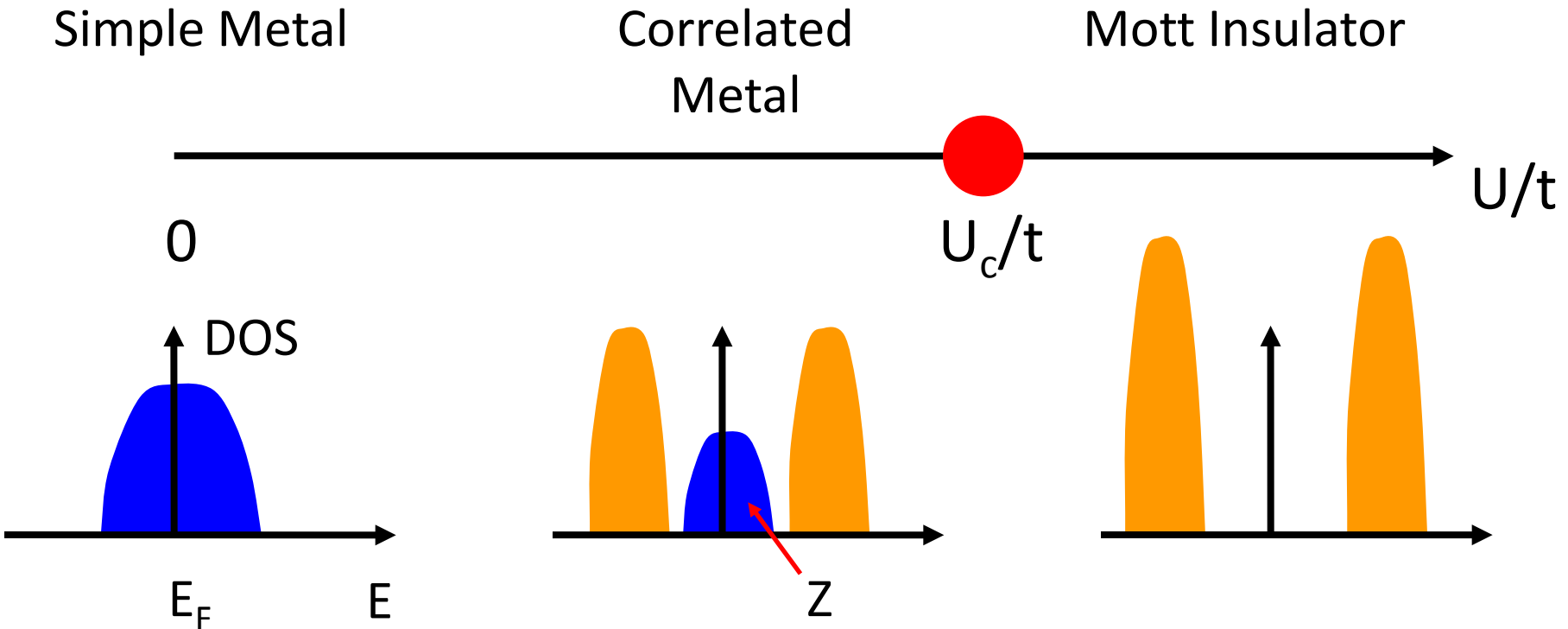
High-spin

$J > \Delta$

$J < \Delta$

Low-spin

Mott Transition



Requiring theoretical tool that is able to access the phases on both sides of the transition

U(1) Slave-Spin Theory

constraint:

$$d_{i\alpha\sigma}^\dagger = S_{i\alpha\sigma}^+ f_{i\alpha\sigma}^\dagger \quad S_{i\alpha\sigma}^z = f_{i\alpha\sigma}^\dagger f_{i\alpha\sigma} - \frac{1}{2}$$

Schwinger boson representation: $S_{i\alpha\sigma}^+ = a_{i\alpha\sigma}^\dagger b_{i\alpha\sigma}$

$$d_{i\alpha\sigma}^\dagger = z_{i\alpha\sigma}^\dagger f_{i\alpha\sigma}^\dagger \quad z_{i\alpha\sigma}^\dagger = P_{i\alpha\sigma}^- a_{i\alpha\sigma}^\dagger b_{i\alpha\sigma} P_{i\alpha\sigma}^+$$

$$\bar{Z}_{i\alpha\sigma} = |\langle z_{i\alpha\sigma} \rangle|^2 \quad P_{i\alpha\sigma}^\pm = 1/\sqrt{1/2 + \delta \pm (a_{i\alpha\sigma}^\dagger a_{i\alpha\sigma} - b_{i\alpha\sigma}^\dagger b_{i\alpha\sigma})/2}$$

Determining renormalization amplitudes:

$$H_f^{\text{mf}} = \frac{1}{2} \sum_{ij\alpha\beta\sigma} t_{ij}^{\alpha\beta} \langle z_{i\alpha\sigma}^\dagger z_{j\beta\sigma} \rangle f_{i\alpha\sigma}^\dagger f_{j\beta\sigma} + \sum_{i\alpha\sigma} (\Delta_\alpha - \lambda_{i\alpha\sigma} - \mu) f_{i\alpha\sigma}^\dagger f_{i\alpha\sigma},$$

$$H_S^{\text{mf}} = \frac{1}{2} \sum_{ij\alpha\beta\sigma} t_{ij}^{\alpha\beta} \langle f_{i\alpha\sigma}^\dagger f_{j\beta\sigma} \rangle z_{i\alpha\sigma}^\dagger z_{j\beta\sigma} + \sum_{i\alpha\sigma} \frac{\lambda_{i\alpha\sigma}}{2} (\hat{n}_{i\alpha\sigma}^a - \hat{n}_{i\alpha\sigma}^b) + H_{\text{int}}$$

RY and Q. Si, PRB **86**, 085104 (2012),

Cf. (Z_2 slave-spin theory): L. de'Medici et al., PRB **72**, 205124 (2005).

Possible Ground States

- Metal:

ordered slave spins ($Z>0$);

gapless electrons (finite electron Fermi surface)

- Mott Insulator

disordered slave spins ($Z=0$);

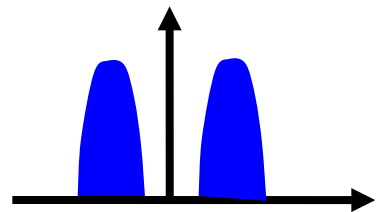
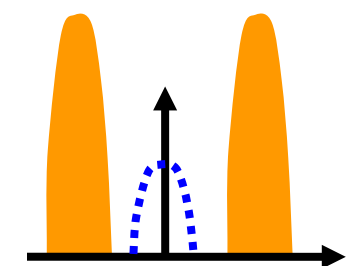
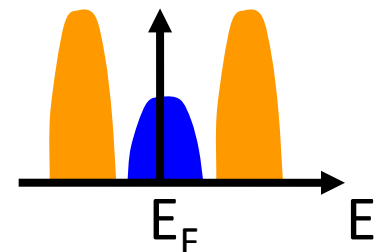
gapless spinons (finite spinon Fermi surface)

- Band Insulator

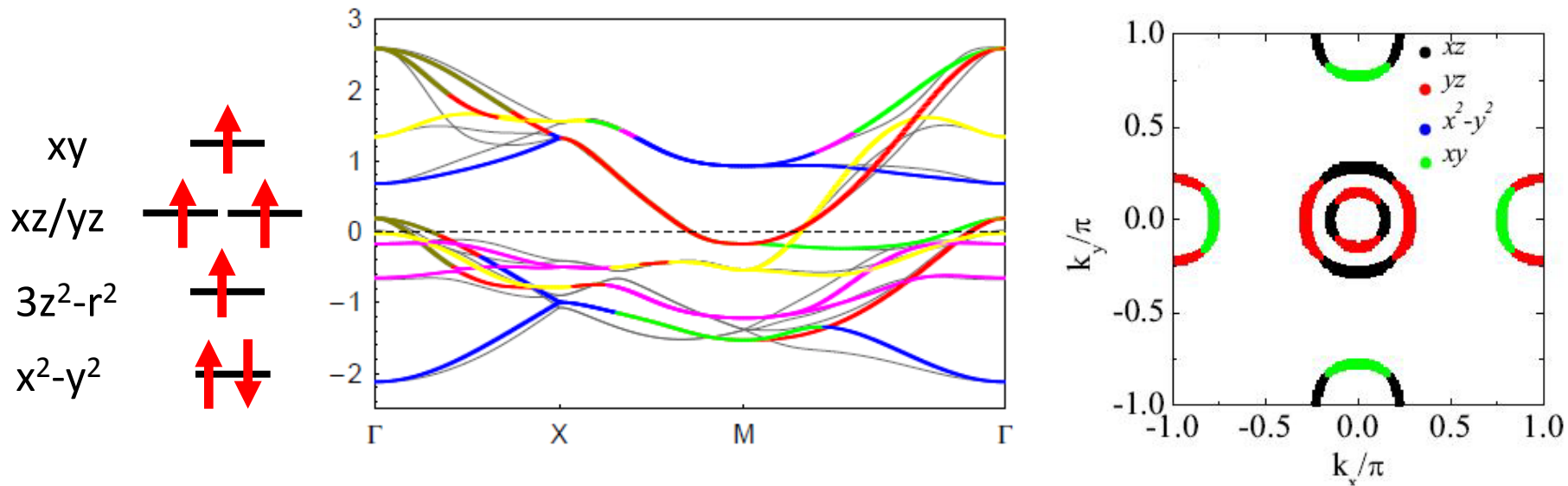
ordered slave spins ($Z>0$);

gapped spinons

gapped electrons



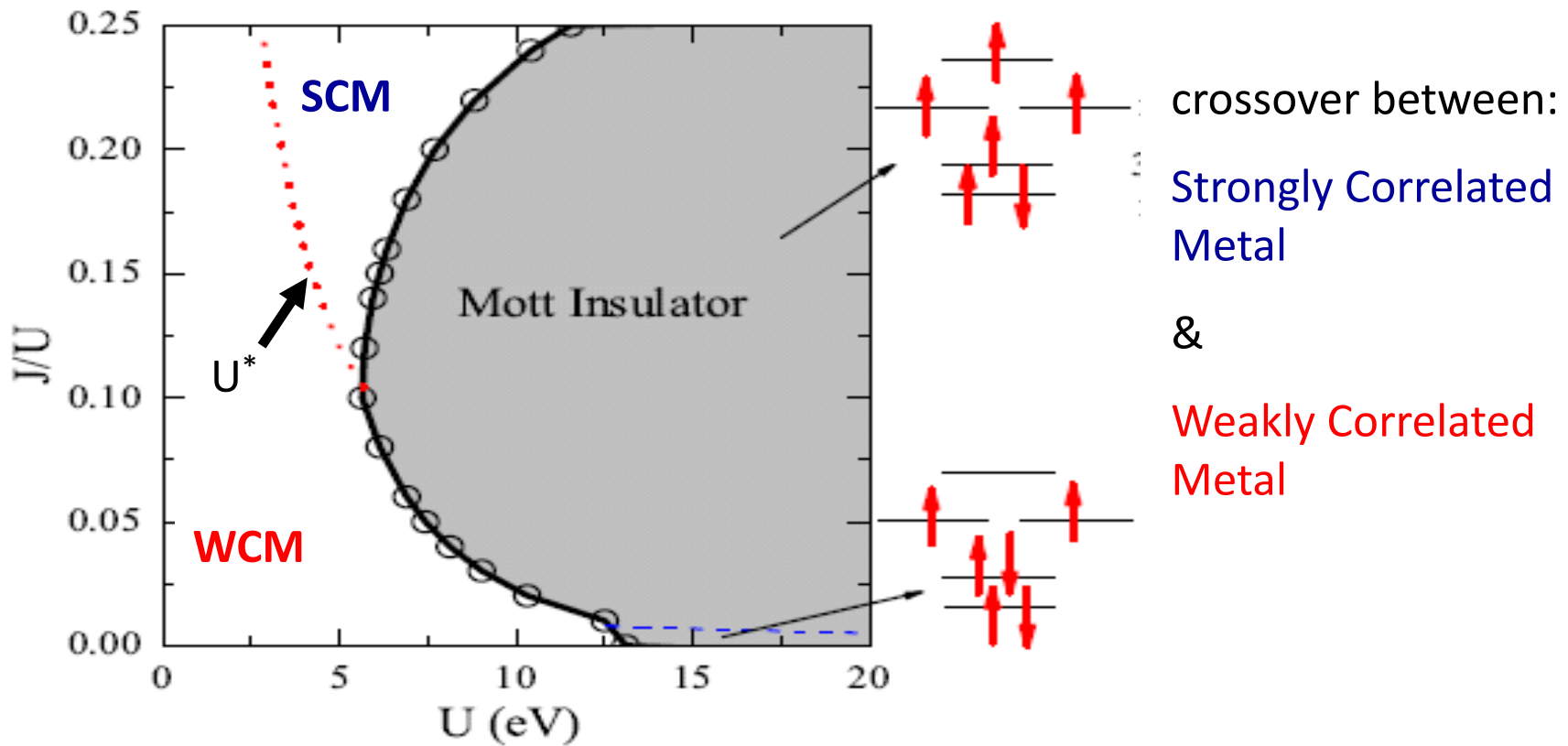
Kinetic Part of the Multiorbital Model for Iron Pnictides



S. Graser et al., New J. Phys. **11**, 025016 (2009).

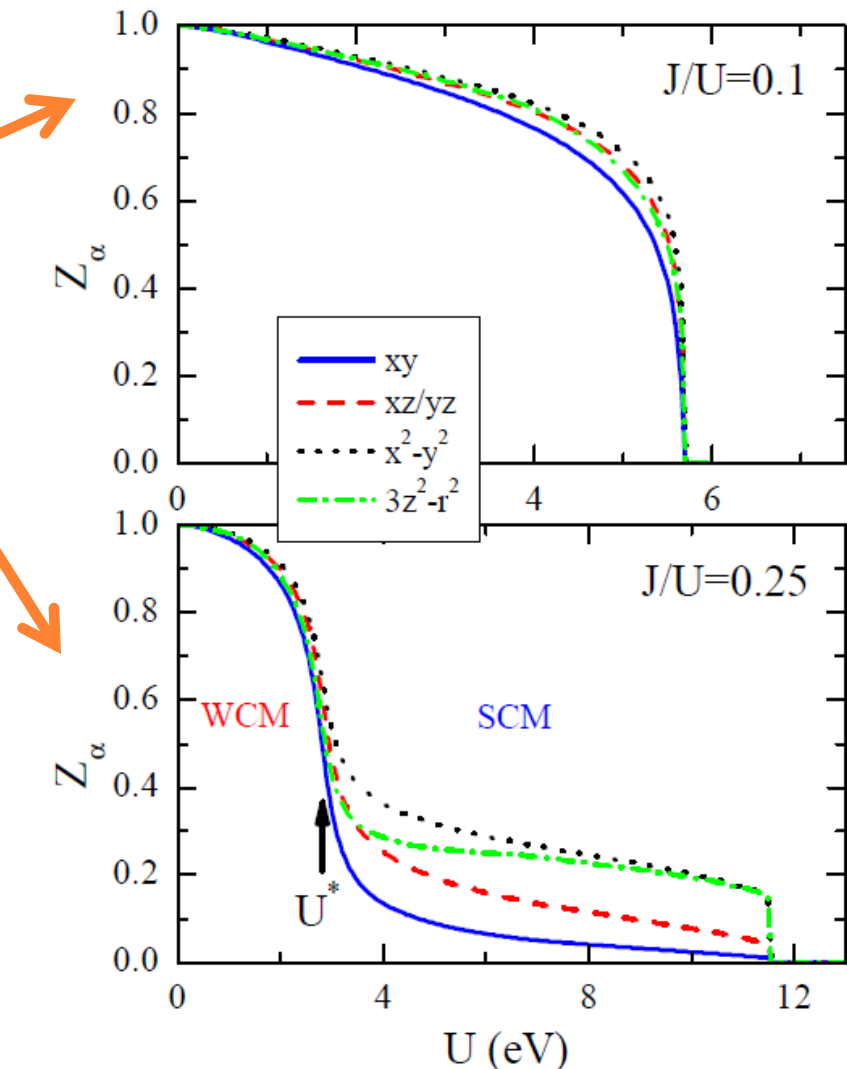
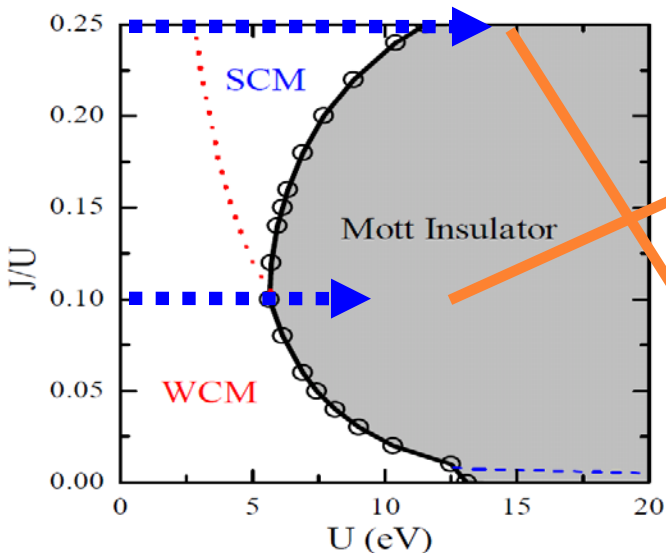
- ✓ tight-binding model involving five Fe 3d orbitals
- ✓ nonzero crystal field splitting
- ✓ double degenerate xz and yz orbitals

Mott Transition in the Five-Orbital Model



RY and Q. Si, PRB **86**, 085104 (2012)

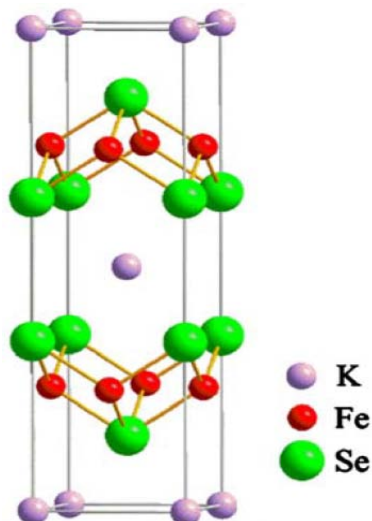
Correlation Effects in Metallic State



SCM:

- Reduced quasiparticle spectral weight, Z
- Strong orbital selectivity

Mott Localization in Alkaline Iron Selenides



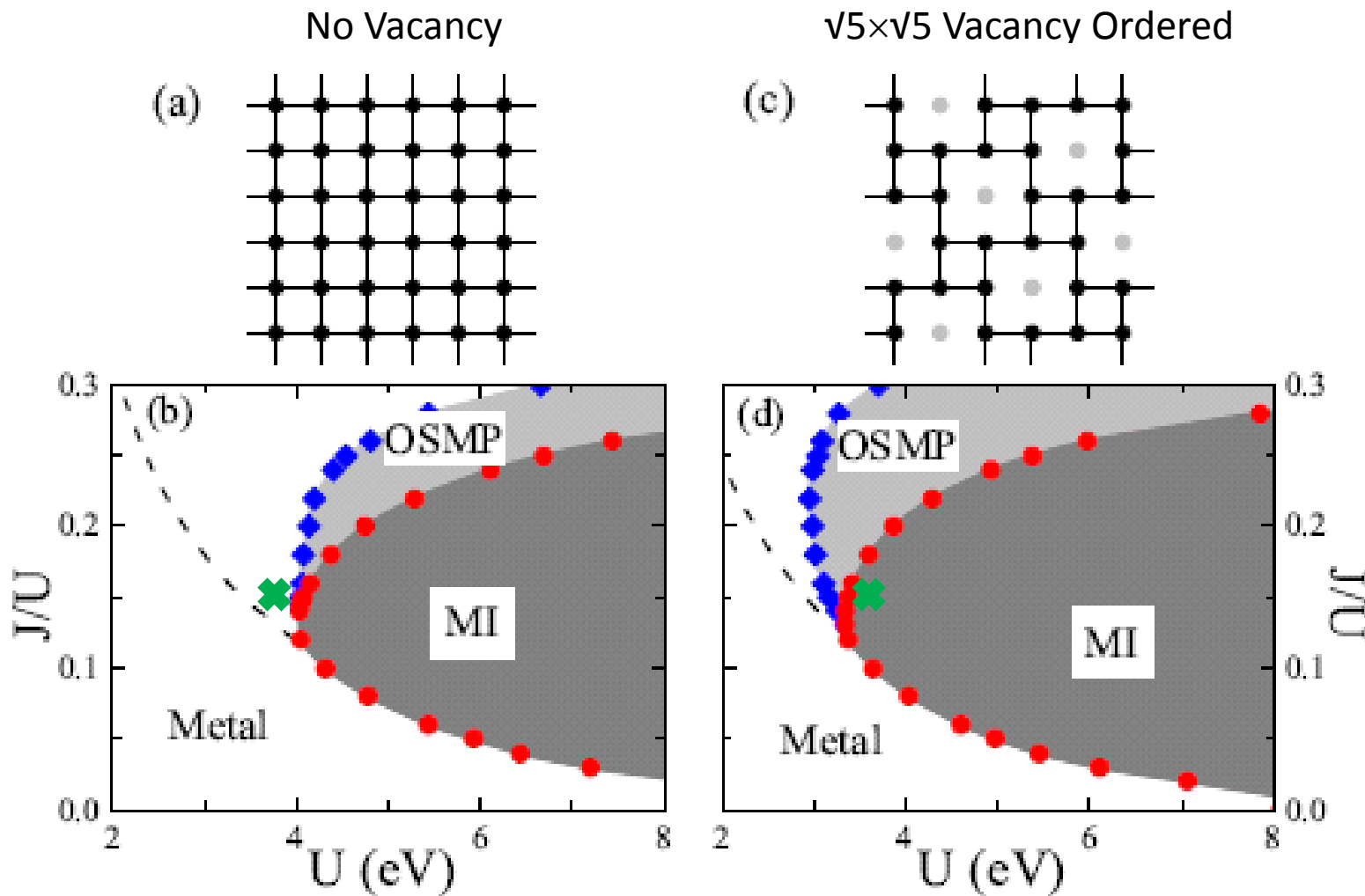
Vacancy Order

vs

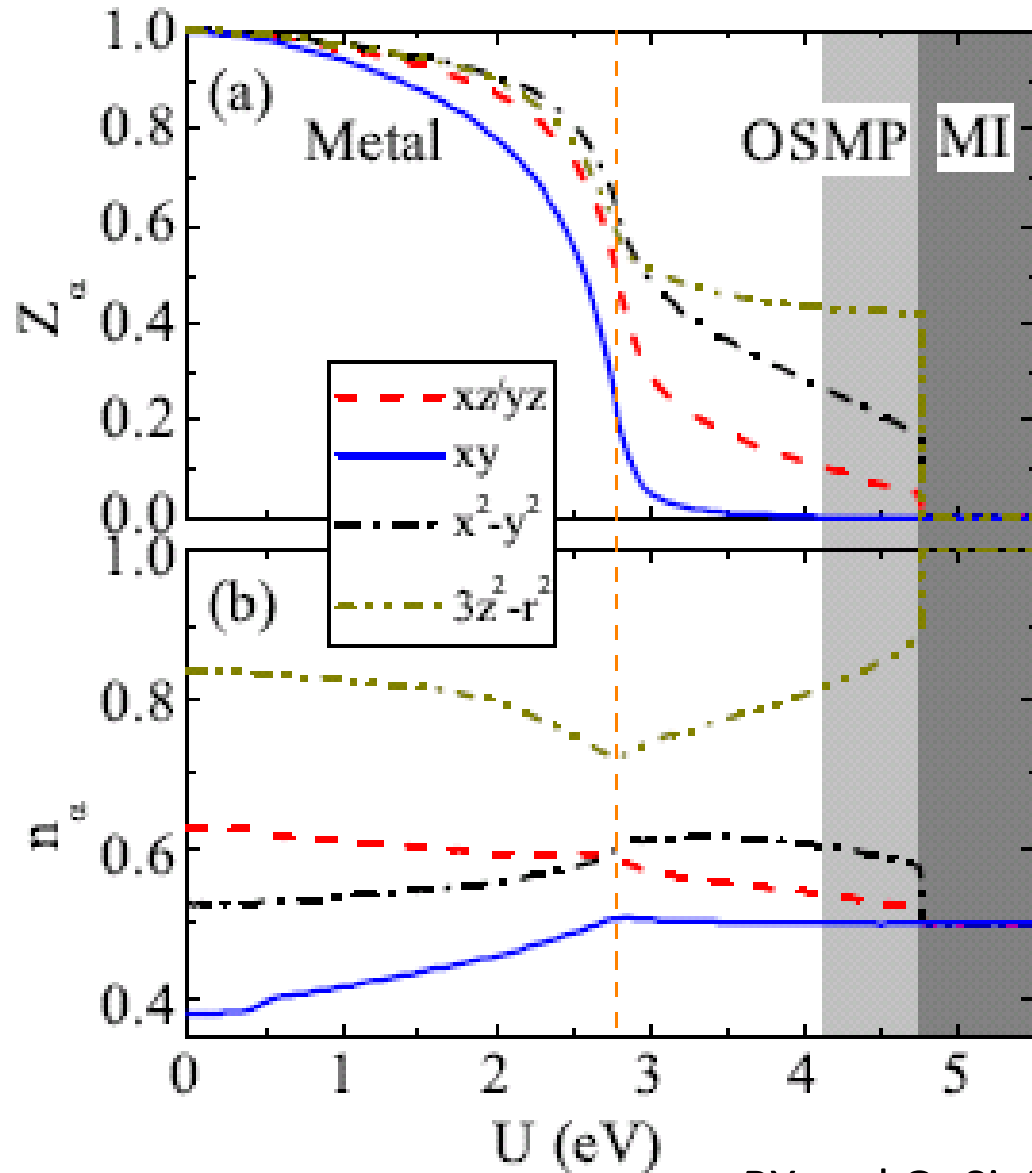
Mott
Localization

Metal-to-Insulator Transition in Parent $K_xFe_{2-y}Se_2$

filling $n=6$ kinetic energy reduction by ordered vacancies



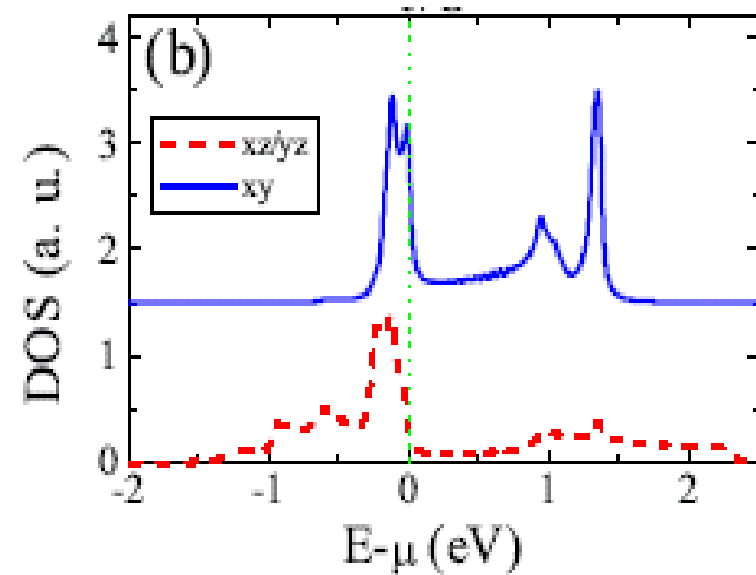
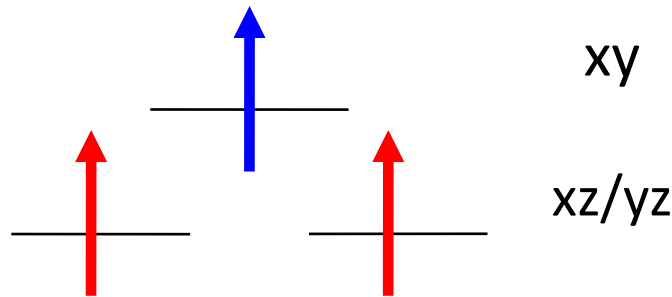
Evolution of QP Weight Z with U



$n=6, J/U=0.2$

OSMP:
xy orbital localized;
others itinerant.

Nature of the Orbital-Selective Mott Phase



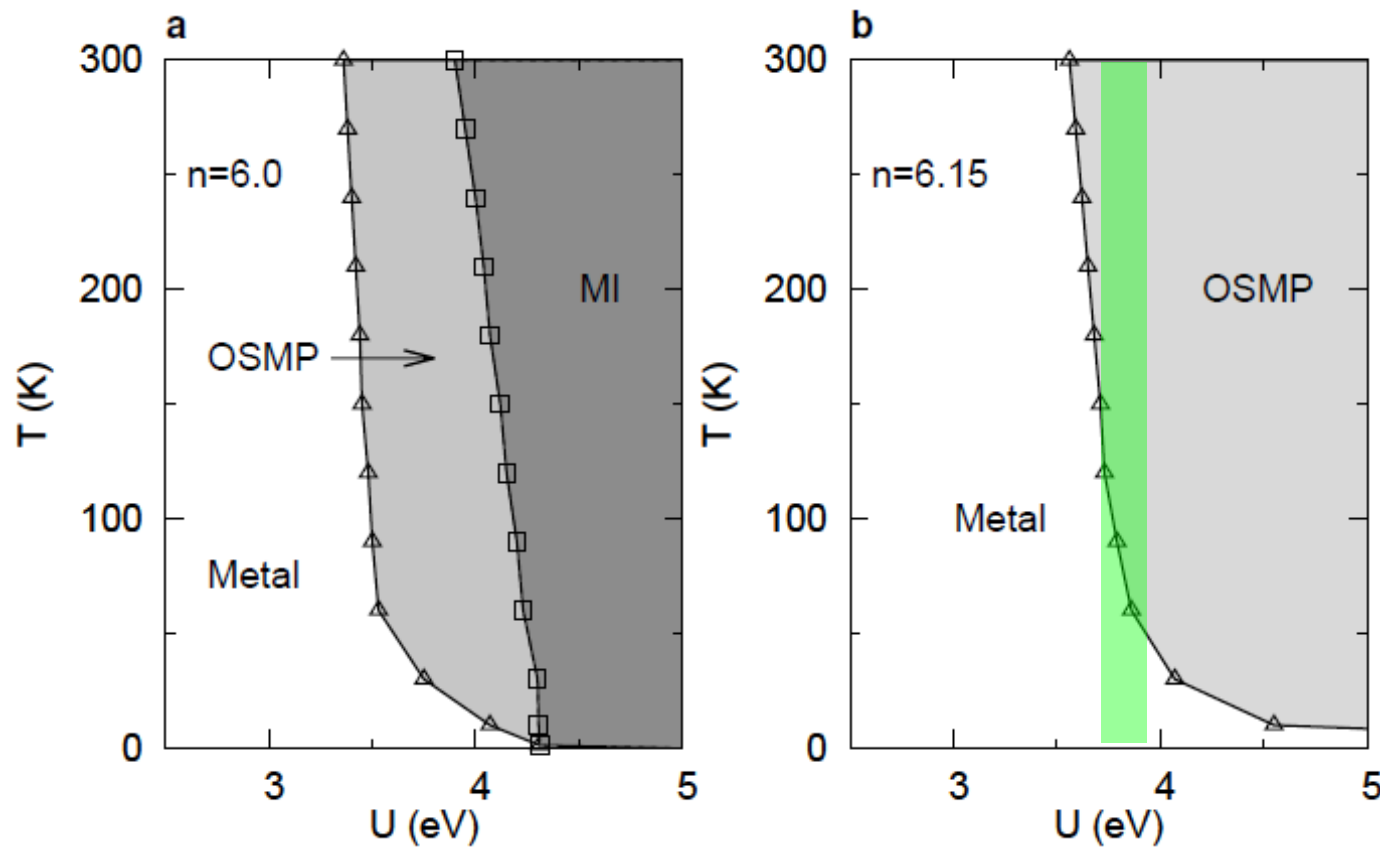
- ✓ crystal level splitting: lowest filling in d_{xy}
- ✓ d_{xy} bands is narrower than d_{xz}/y_z bands
- ✓ Hund's coupling reduces orbital fluctuations

Cf. (other contexts/regimes):

Anisimov et al, Eur. Phys. J. B **25**, 191 (2002);

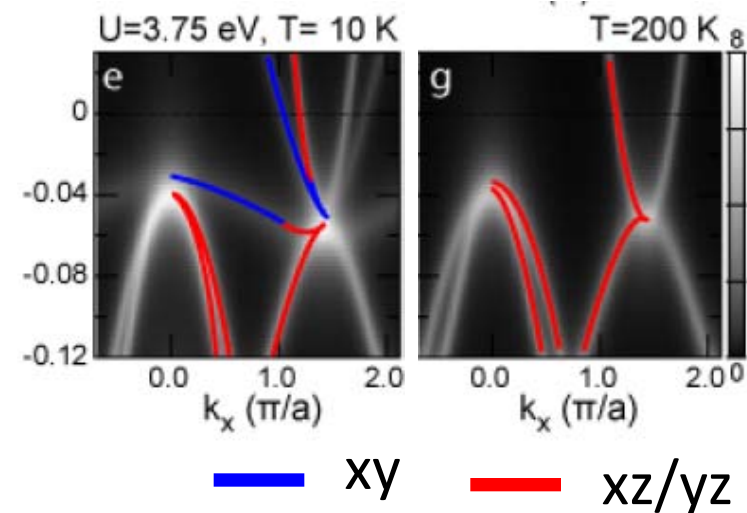
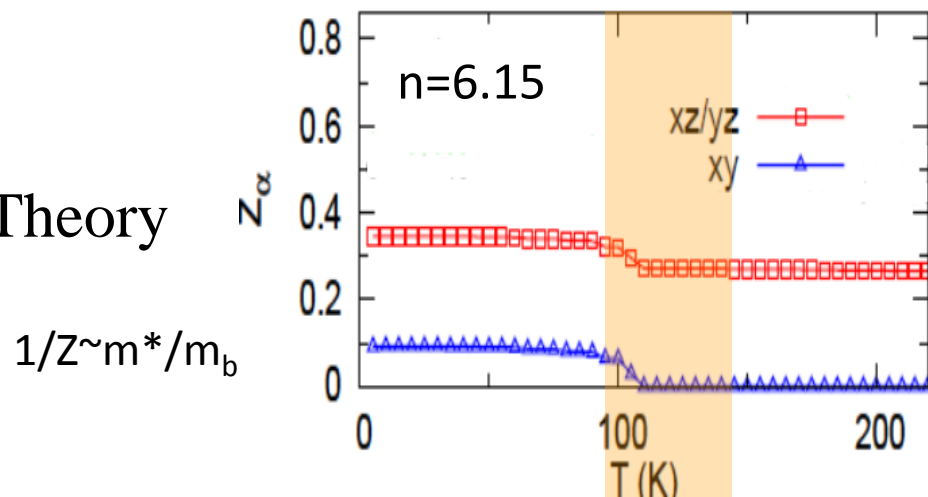
de' Medici et al, PRL **102**, 126401 (2009).

Temperature Induced Mott Localization

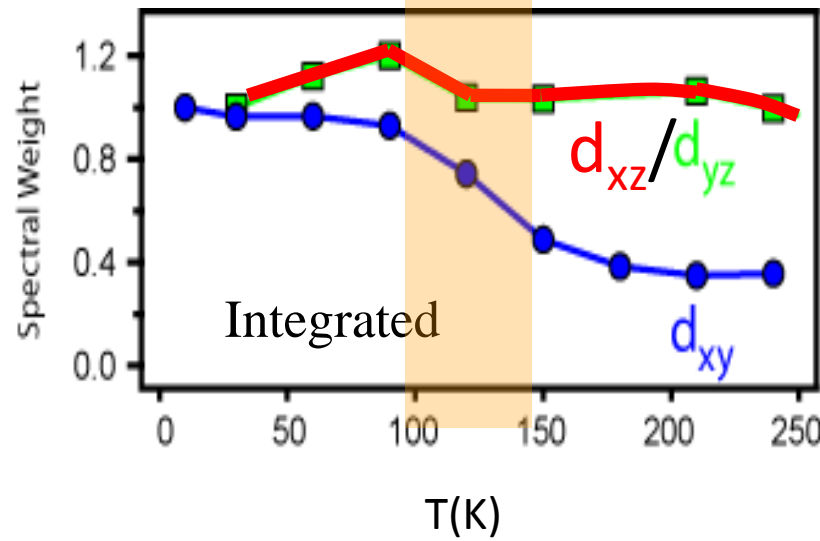


Temperature Induced OSMT in $K_xFe_{2-y}Se_2$

Theory



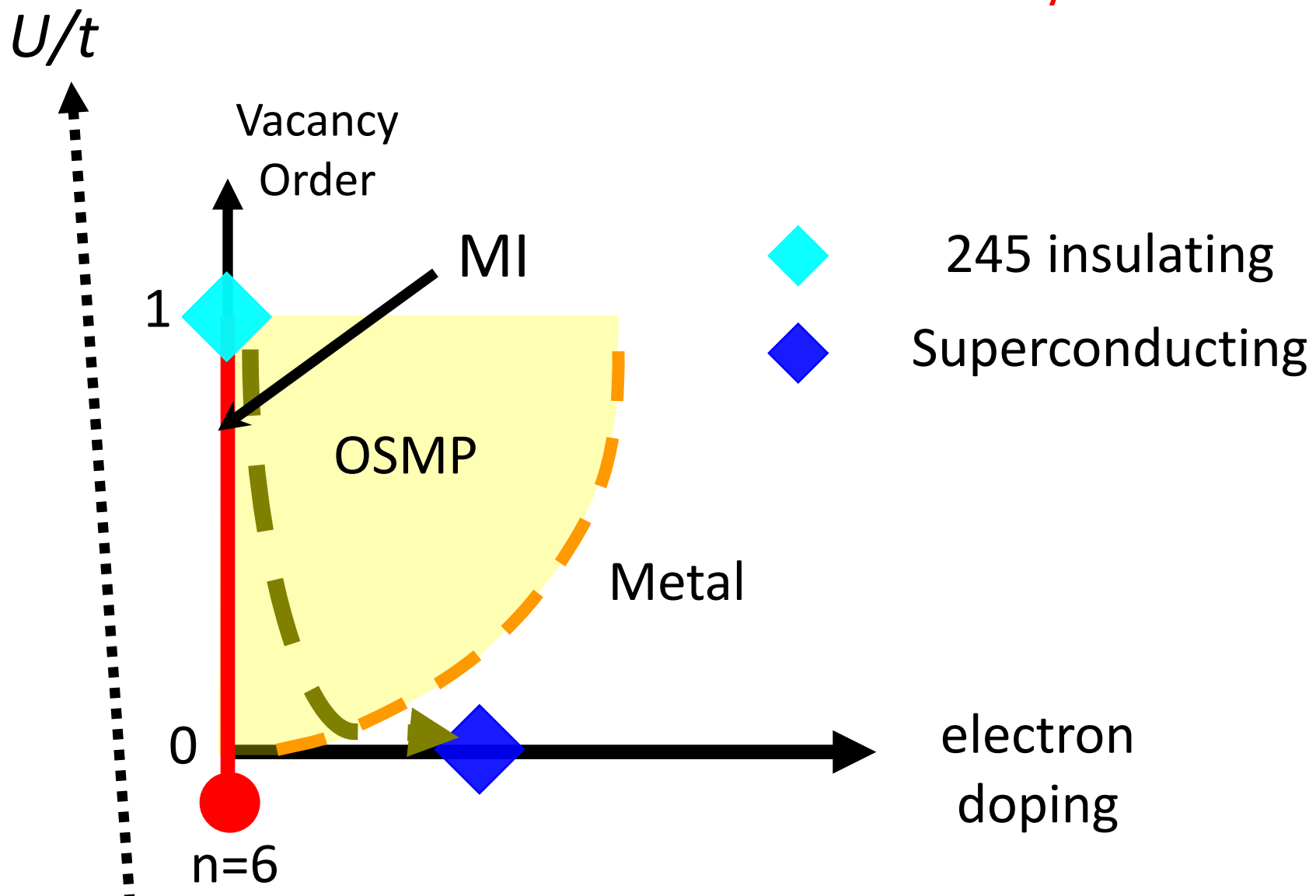
ARPES



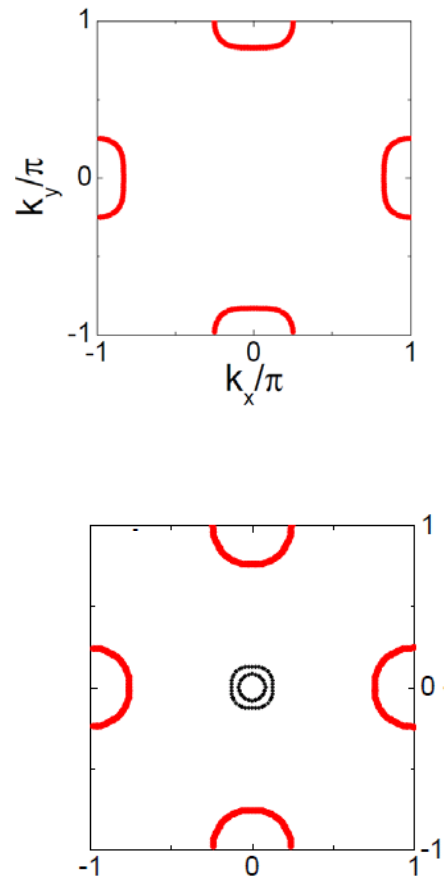
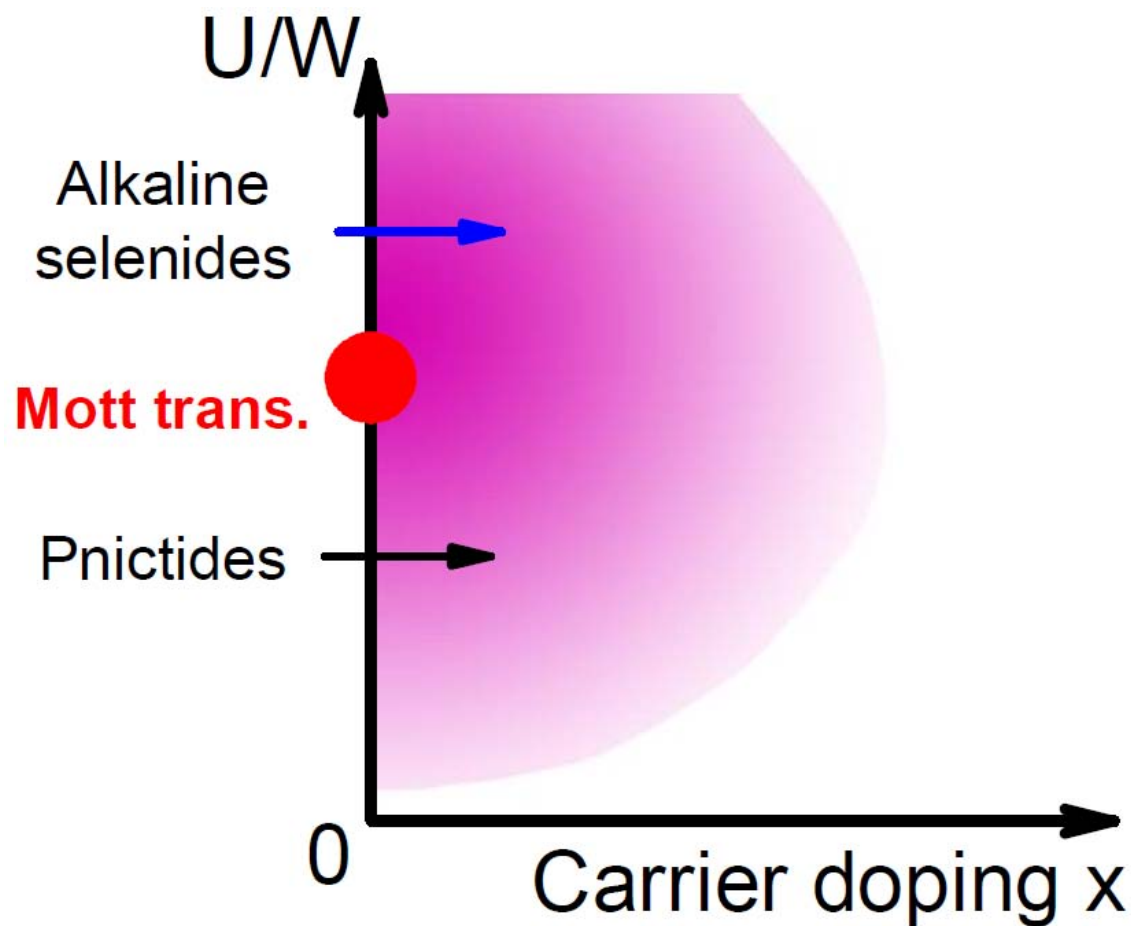
M. Yi, RY, et al., PRL **110**, 067003 (2013)

- Similar strong orbital selective behavior also observed in single-layer FeSe/STO (M. Yi's talk on Monday)

Phase Diagram for $A_xFe_{2-y}Se_2$



A Unified Phase Diagram



comparable T_c for iron pnictides & alkaline iron selenides

Effective Exchange Interactions near a Mott Transition

- One band Hubbard model

$$H = \sum_{(ij),\sigma} t_{ij} d_{i\sigma}^+ d_{j\sigma} + U \sum_i n_{i\uparrow} n_{i\downarrow}$$

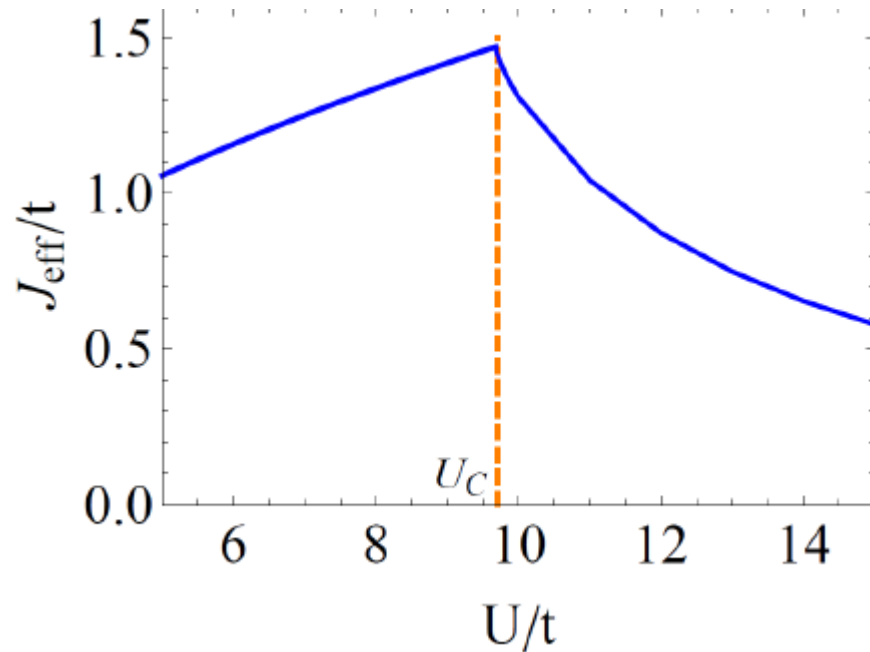
- Slave rotor representation

$$d_{i\sigma} = e^{-i\theta_i} f_{i\sigma}$$

S. Florence and A. Georges,
Phys. Rev. B **70**, 035114 (2004).

- Effective exchange couplings among spinons

$$H_{\text{ex}} = J_{\text{eff}} f_{i\sigma}^+ f_{i\sigma'}^+ f_{j\sigma'}^+ f_{j\sigma}$$



W. Ding et al., unpublished.

Superconducting pairing in multiorbital t-J₁-J₂ model

$$H = - \sum_{i < j, \alpha, \beta, s} t_{ij}^{\alpha\beta} c_{i\alpha s}^\dagger c_{j\beta s} + h.c. - \mu \sum_{i, \alpha} n_{i\alpha}$$
$$+ \sum_{\langle ij \rangle, \alpha, \beta} J_1^{\alpha\beta} \left(\vec{S}_{i\alpha} \cdot \vec{S}_{j\beta} - \frac{1}{4} n_{i\alpha} n_{j\beta} \right) + \sum_{\langle\langle ij \rangle\rangle, \alpha, \beta} J_2^{\alpha\beta} \left(\vec{S}_{i\alpha} \cdot \vec{S}_{j\beta} - \frac{1}{4} n_{i\alpha} n_{j\beta} \right)$$

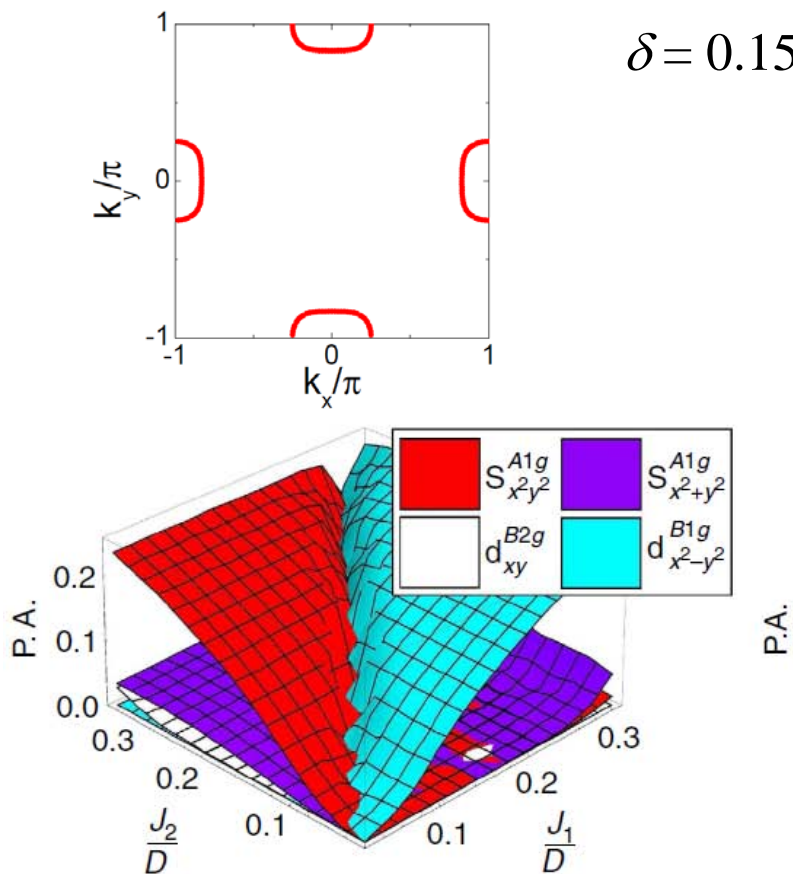
- ✓ decomposing the J₁, J₂ interactions in pairing channels
- ✓ intra-orbital singlet pairings
- ✓ do not address coexistence of SC and AFM

P Goswami et al., *EPL* **91**, 37006 (2010)

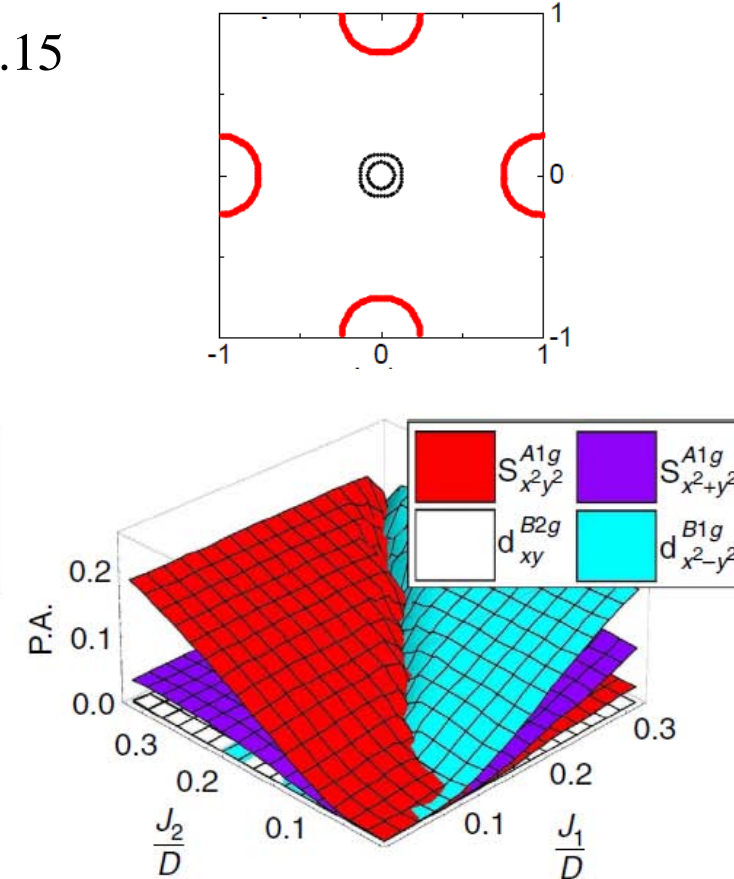
RY et al., *Nat Commun* **4**, 2783 (2013)

Comparable Pairing Amplitudes

Alkaline iron selenide

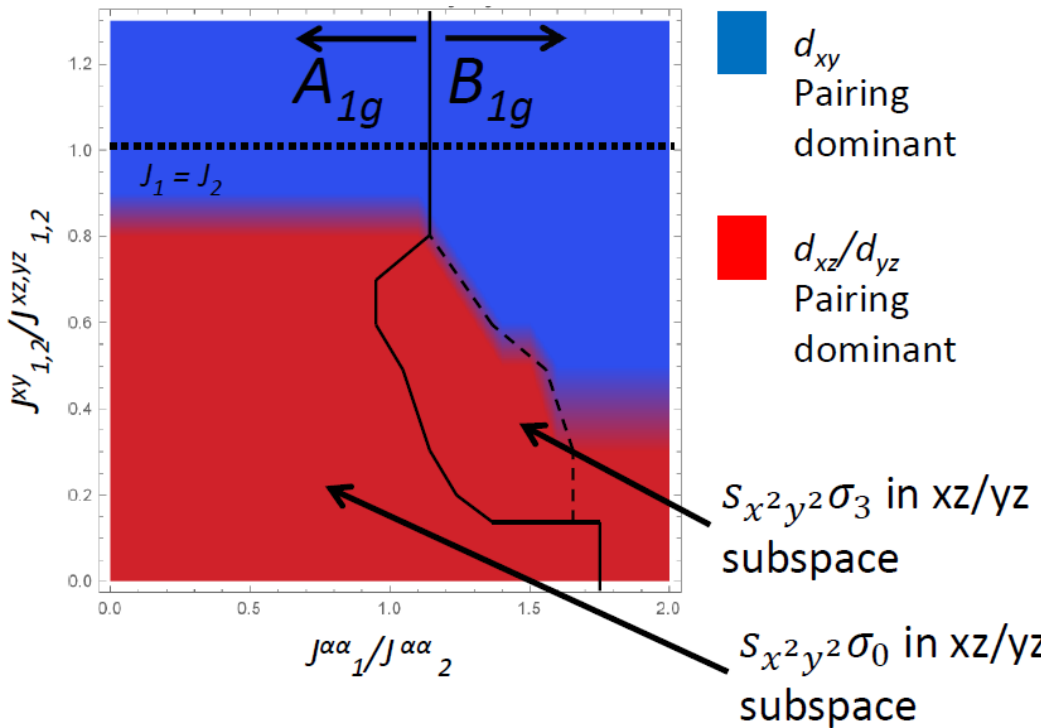


Iron pnictide



➤ Similar results also for 1-layer FeSe/STO

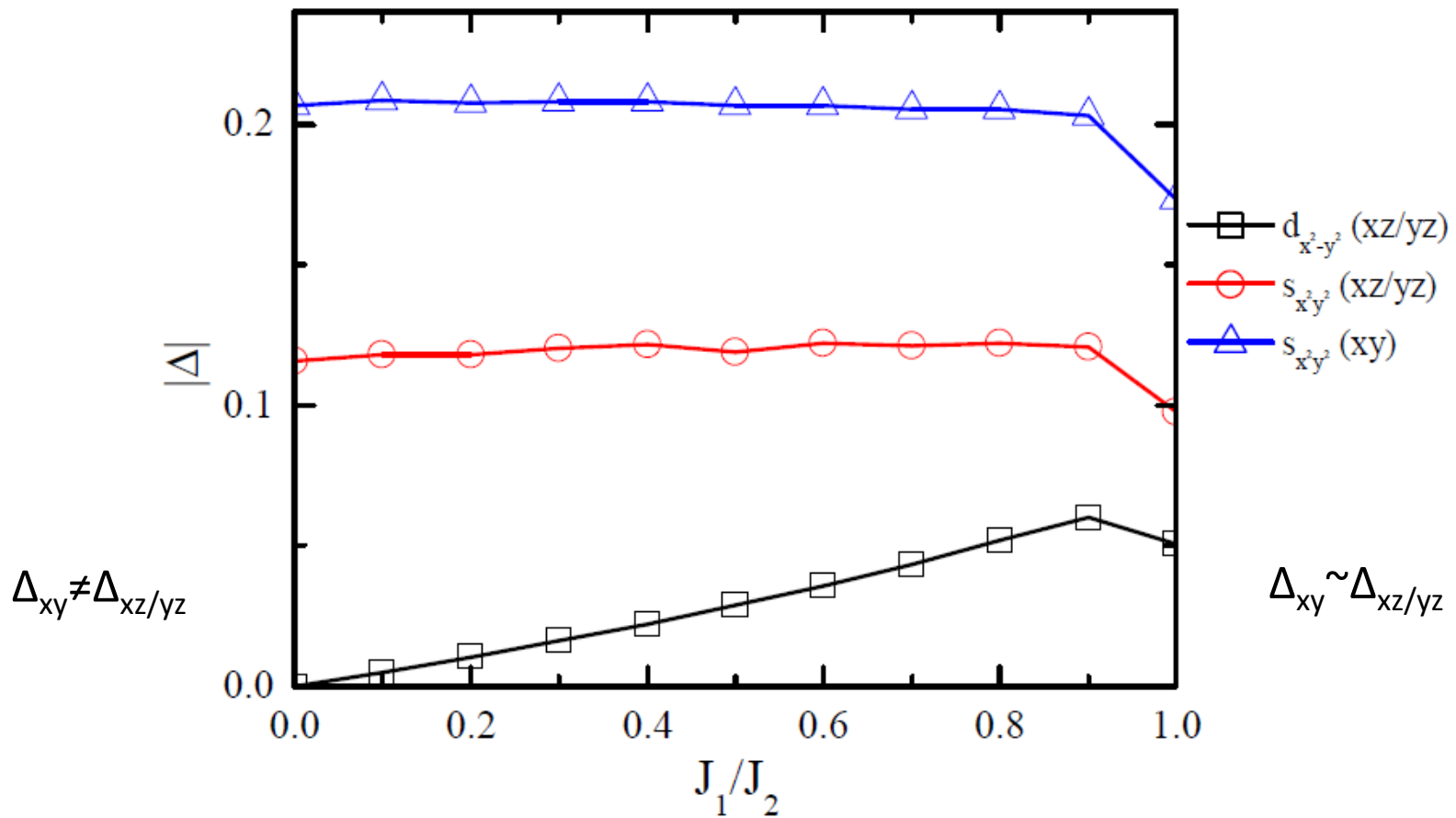
Orbital-Selective Pairing in Multiorbital t-J₁-J₂ model



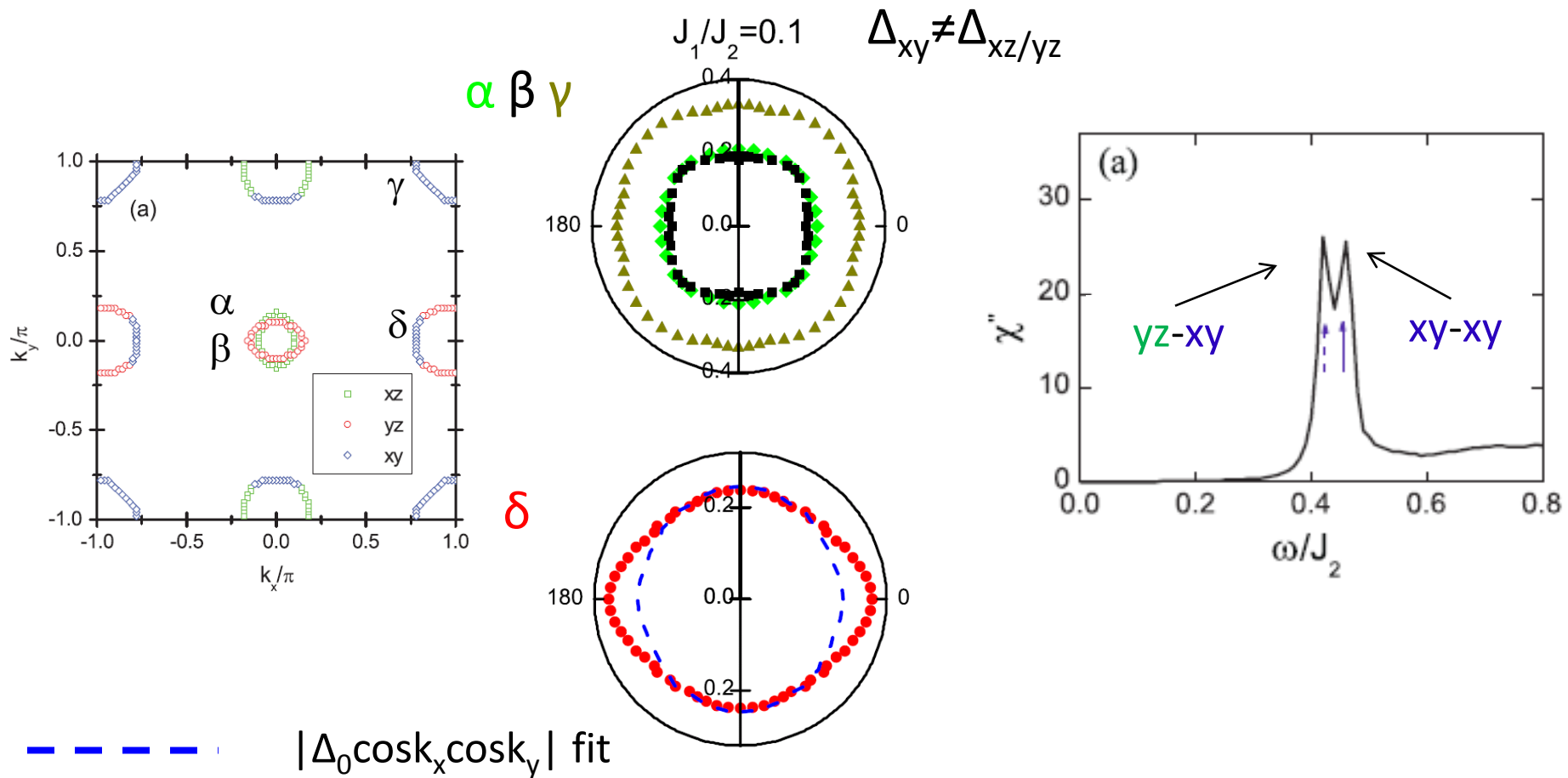
- ✓ diagonal but orbital dependent J matrix, $r_O = J_{1(2)}^{xy} / J_{1(2)}^{xz/yz}$
- ✓ competition between s-A_{1g} and d-B_{1g} pairing channels
- ✓ s-B_{1g} pairing stabilized at intermediate r_O .

Orbital-Selective Pairing Amplitudes

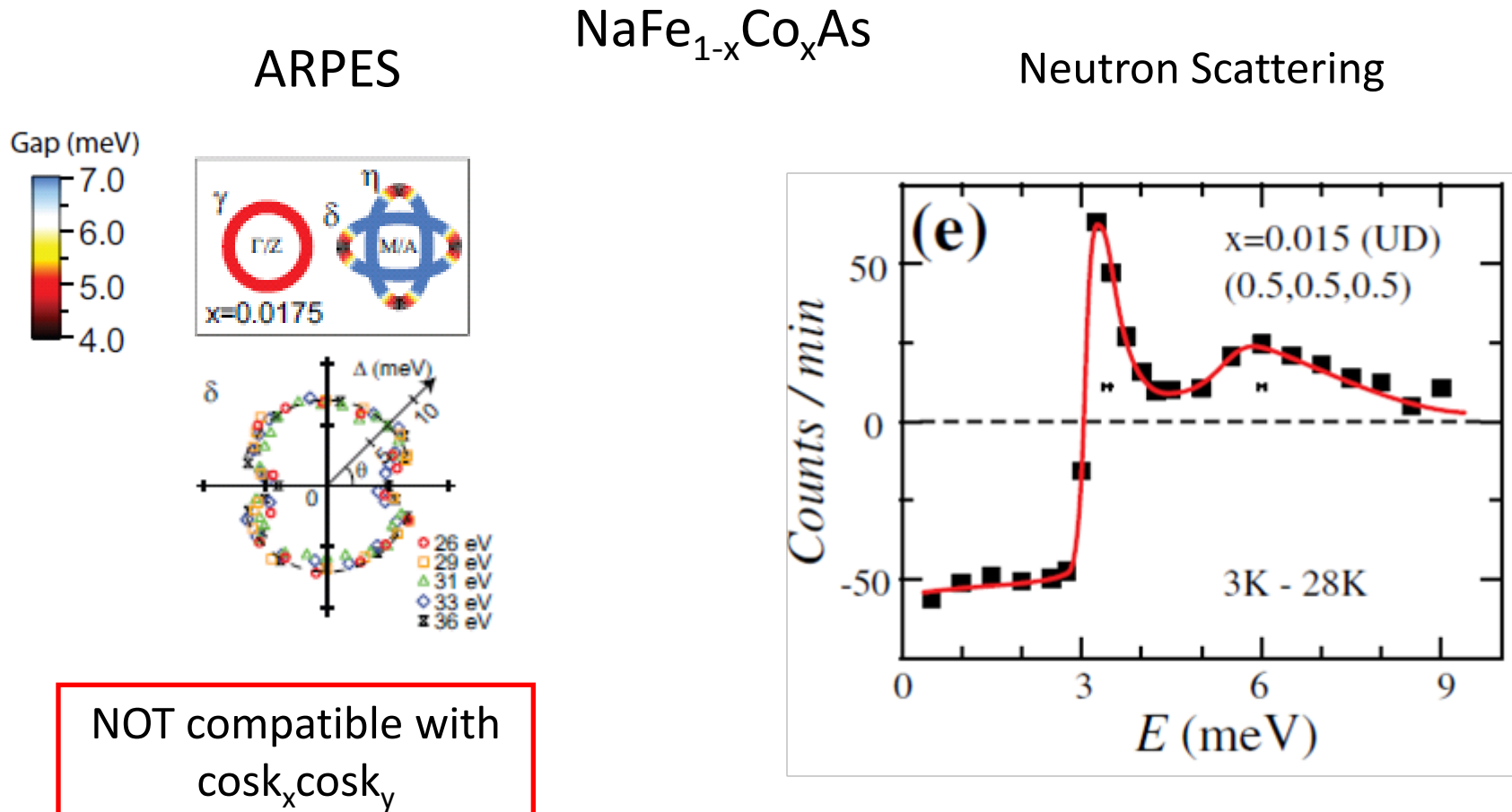
Dominant pairing channels with A_{1g} symmetry at $r_O=1$



Anisotropic Superconducting Gap and Splitting of Spin Resonance Peaks



Anisotropic SC Gap and Double Spin Resonances in underdoped Na 111



Q Q Ge et al., *PRX* **3**, 011020 (2013)

C Zhang, RY et al., *PRL* **111**, 207002 (2013)

Summary

- Metal-to-Mott-insulator transition studied by slave-spin method in multi-orbital Hubbard models for iron-based superconductors
- Mott localization influenced by various factors: Hund's coupling, Fe vacancy order, crystal level splitting ...
- Strong **orbital-selective Mott** physics in iron chalcogenides
- **Comparable pairing amplitudes** for iron pnictides and alkaline iron selenides
- **Strong orbital dependent superconducting pairing**: gap anisotropy and splitting of neutron resonance in the superconducting state